Quantitative assessment of the oxygen isotope composition of fish otoliths from Lake Mungo, Australia

Kelsie Long[1,2*], David Heslop[1], Eelco Rohling[1]

[1]Research School of Earth Sciences, Australian National University, 142 Mills Rd, Canberra, ACT, 2601

[2]Present address: School of Culture, History and Language, Australian National University, H.C.Coombs, 9 Fellows Rd, Canberra, ACT, 2601

*Corresponding author:

Email: Kelsie.long@anu.edu.au,

Postal address: Archaeology and Natural History, H.C.Coombs, 9 Fellows Road, Canberra, ACT 2601, Australia

Keywords: Quaternary, oxygen isotopes, Willandra Lakes, otoliths, arid zone

15 **ABSTRACT**

16 The Willandra lakes are a series of once interconnected and now-dry lake basins in the
17 arid zone of south-eastern Australia. They are sites of cultural, archaeological and
18 geological significance preserving records of Aboriginal occupation and environmental
19 change stretching back at least 50 thousand years. Linking the archaeology with the
20 palaeoenvironment is complicated by the millennial time spans represented by the
21 sedimentary hydrological record versus the sub-decadal evidence of each archaeological
22 site. Oxygen isotope records across annual growth rings of fish otoliths (ear stones) can
23 elucidate flooding and drying regimes on sub-annual scales. Otoliths from hearth sites
24 (fireplaces) link lake hydrology with people eating fish on the lakeshore. Previous
25 interpretations of oxygen isotopic trends in Last Glacial Maximum (LGM) hearth otoliths
26 were interpreted in terms of high evaporation under dry conditions. However, this ignored
27 hydrology-driven changes in water $\delta^{18}O$. Here, a mass balance model is constructed to
28 test what effect lake desiccation would have on water $\delta^{18}O$ and how this compares with
29 LGM otolith records. Based on this modelling, we suggest that Lake Mungo otolith
30 signatures are better explained by evaporation acting on full lakes, rather than by lake
31 drying.

INTRODUCTION AND BACKGROUND

Lake Mungo is one of a series of now-dry lake basins that make up the Willandra Lakes World Heritage Area in arid south-eastern Australia (Fig. 1). It is one of the earliest archaeological sites in Australia and the site of the oldest human cremation and ritual ochre burial in the world (Mungo I and III) dated to 41 ± 4 ka (Bowler et al., 2003; Olley et al., 2006). A key feature of Lake Mungo are the lakeside sand and clay dunes (lunettes) which preserve a sedimentary record of alternating wet and dry conditions over the past 100 thousand years (Bowler, 1998; Bowler et al., 2012; Fitzsimmons et al., 2014; Jankowski et al., 2020). As these lunettes formed, they covered and preserved archaeological material preserving a record of past life and environments. The relationship between periods of human occupation and palaeoenvironmental changes has been a major research theme in the area, with initial studies predominantly concentrating on the stratigraphy and archaeology preserved at the southern tip of the Mungo lunette (Bowler et al., 1970; Bowler, 1998). More recent work, conducted as part of the ongoing Mungo Archaeology Project (MAP), has focused on the Central Lunette area, where widespread erosion has uncovered an array of stratigraphic units and archaeological features (Fitzsimmons et al., 2014; Stern, 2015; Barrows et al., 2020; Jankowski et al., 2020). Among these archaeological traces are thousands of fish otoliths that, when found in hearth sites (cooking fireplaces), provide an opportunity to link conditions in the lake directly with Aboriginal presence on the lake shore.

Otoliths grow within the inner ears of bony fish through the incremental deposition of calcium carbonate (aragonite) in periodic, usually annual, rings (Campana, 1999). The oxygen isotope ($\delta^{18}O$) composition of fish otoliths is controlled by the temperature and

55 $\delta^{18}O$ of the water in which the fish lived. The δ notation used here represents the ratio of
56 ^{18}O to ^{16}O relative to that in a standard material, Vienna Pee Dee Belemnite (VPDB) for
57 carbonates (otoliths) and Vienna Standard Mean Ocean Water (VSMOW) for water. If the
58 ambient water $\delta^{18}O$ remains constant, a change of 1‰ in otolith $\delta^{18}O$ values would reflect
59 a ~4°C change in water temperature (Kalish, 1991). In marine settings where water
60 oxygen isotopes are fairly stable over time, seasonal temperature changes can be
61 detected in the otolith and other biogenic carbonate oxygen isotopes (Weidman and
62 Millner, 2000; Andrus et al., 2002; Mannino et al., 2008; Geffen et al., 2011). At freshwater
63 sites, the $\delta^{18}O$ of ambient water is more variable, changing with precipitation, flooding
64 and evaporation. These water composition changes tend to dominate the $\delta^{18}O$ record of
65 otoliths and other carbonate remains in freshwater environments (Leng and Marshall,
66 2004; Leng and Lewis, 2014; Dufour et al., 2018; Long et al., 2018). Therefore,
67 consideration of the hydrological controls inherent within the system as a whole is crucial
68 for the correct interpretation of the geochemical traces preserved in otoliths.

69 Some (e.g. Allen and Holdaway, 2009), have described the Willandra Lakes as so lacking
70 in surface water and so windy and dusty that the region was uninhabited during the Last
71 Glacial Maximum, which spanned roughly 31 to 19 thousand years. However, the
72 alternating sands and clays of the Lake Mungo lunette that formed during the LGM
73 suggest that lake levels varied between wet periods following floods, and periods of drying
74 that exposed at least part of the lake floor (Bowler et al., 2012; Fitzsimmons et al., 2014;
75 Stern, 2015). Likewise, the abundance of stone tools, hearth sites and other
76 archaeological materials found within LGM-aged dunes indicate at least periodic human
77 presence (Stern et al., 2013; Fitzsimmons et al., 2014; Stern, 2015). The question arises

78 whether human occupation on the lakeshores coincided with periods of low lake level,
79 wetter phases or both? Was the lake stable or periodically drying out completely and then
80 refilled by flood waters and how do these changes track with Aboriginal presence on the
81 lakeshore? Interactions between climate, lake hydrology and Aboriginal peoples remain
82 difficult to disentangle with current evidence the issue is complicated by mismatch
83 between the millennial time spans represented by the sedimentary hydrological record,
84 and the sub-decadal evidence represented by each archaeological site, some of which
85 are the remains of a single meal. The MAP is continuing to conduct rigorous and
86 systematic recording, dating and assessing of archaeological remains and their
87 associated sediments in partnership with the three traditional groups of the Willandra
88 region: Paakantji (Barkindji), Ngiyampaa and Mutthi Mutthi. As part of the MAP, otoliths
89 recovered from Aboriginal hearth sites offer an opportunity to examine water conditions
90 at Lake Mungo during the LGM in greater detail and on timescales commensurate with
91 human lives.

92 In a previous study (Long et al., 2014), oxygen isotopes and trace elements were
93 analysed across the age increments of fish otoliths recovered from a series of Aboriginal
94 hearth sites at Lake Mungo dating to the LGM (19,490 – 19,330 and 19,420 – 19,220 cal
95 yr BP at 95.4% probability). The hearth otoliths all showed an increasing trend in both
96 Sr/Ca ratios and oxygen isotopes (Fig. 2). Increases in Sr/Ca ratios are typically linked
97 with fish movements to regions of high salinity (Zimmerman, 2005; Kerr et al., 2007;
98 Macdonald and Crook, 2010). Moreover, preferential ^{16}O removal during evaporation
99 causes water $\delta^{18}O$ to increase (Washburn and Urey, 1932; Craig et al., 1963) which would
100 be recorded in the fish otoliths. The results, therefore, seemed to support the “easy prey

hypothesis" proposed by Bowler (1998), whereby the fish entered into Lake Mungo with, or after, a flood, and subsequently became trapped by evaporative conditions that cut off Lake Mungo from the rest of the Willandra system. It was then hypothesized that the trapped fish were targeted by human occupants, who took advantage of an assumed high-salinity induced supine state of the fish, to "scoop [them] up in shallow waters" (Bowler, 1998, p. 148). Other LGM records also suggest that it was a cooler, drier and dustier period in Australia (McTainsh and Lynch, 1996; Hesse et al., 2004; Barrows et al., 2007; Reeves et al., 2013). In combination, these factors and the otolith records were interpreted as evidence for strong evaporation, increasing salinity and a drop in lake levels at Lake Mungo (Long et al., 2014). However, this interpretation did not take into account mass balance effects, which could shed light on the relative roles of water inflow and evaporation on changes in the isotopic composition of the water and hence the otoliths.

Isotopic mass balance models provide a theoretical framework to simulate and quantitatively interpret isotopic signals in lakes (Gibson et al., 2016). Under constant forcing, a closed lake will eventually reach a steady state in its mass balance if the volumes of water lost via evaporation and inflowing water are equal. Yet, volumetric mass balance does not equate to isotopic mass balance because this also depends on the mean isotope (δ) values of evaporating and inflowing water fluxes (F_E and F_{in}, respectively) following the generalised form $\delta_L = (V_L\delta_L + F_{in}\delta_p + F_E\delta_E) / (V_L + F_{in} + F_E)$ where δ_E is a function of δ_L via isotopic fractionation (e.g. Dinçer, 1968; Gonfiantini, 1986; Gibson et al., 1996; Gibson and Edwards, 2002; Jones et al., 2005; Rohling, 2016; Lacey and Jones, 2018). These studies use models that combine mass balance and isotopic

mass balance to quantitatively assess the relative influence of different parameters on the isotopic composition of the water, and can provide updated interpretations of archaeological and sediment records. For example, coupled isotope and mass balance models for Lake Ohrid, one of the oldest and deepest lakes in Europe, suggest that precipitation was up to 26% higher during the early Holocene than in the present day, and 44% lower during the LGM (Lacey and Jones, 2018). The application of such models was also able to show that even though rainfall was much lower during the LGM it was still high enough over the lake to support arboreal vegetation and provide a refugium for people during this time (Lacey and Jones, 2018).

In another example, this time focused on drought interpretations from sediment records, Rohling (2016) used mass balance models to test the assumption that if a lake isotope record suggested regional drying then it indicated a period of poor crop yields for farmers nearby. The study demonstrated that crop-growing potential could actually be improving when the lake records (usually inferred from oxygen isotope ratios) suggest that water levels were dropping. This study highlights the need to consider the different hydrological fluxes, catchments, and surface areas, relevant to, lakes versus fields when inferring drought events from sedimentary lake records. Quantitative modelling of lake systems is an essential tool for revealing setting-specific relationships and controls on water $\delta^{18}O$ and improving archaeological and environmental interpretations (Jones, 2013; Gibson and Reid, 2014; Jones et al., 2016; Rohling, 2016).

To date, no mass-balance modelling of the relationship between $\delta^{18}O$ and changes in palaeolake systems has been conducted for the Willandra Lakes. Unlike the lakes of the modelling studies cited above (Jones et al., 2005; Rohling, 2016; Lacey and Jones, 2018),

147 Lake Mungo contains no modern water to measure fluxes and properties, nor hydrological
148 patterns to observe. Given that such currently dry lakes lack surface water, quantitative
149 modelling in palaeolake systems relies on certain assumptions. While observations from
150 nearby river systems can be used to approximate source-water $\delta^{18}O$ for the model,
151 humidity over the lake surface and hence the precise $\delta^{18}O$ of evaporated vapour is
152 unknown. Despite these limitations, simple models can be used to test proposed past
153 hydrological scenarios for physical consistence and to estimate at least the sign and order
154 of magnitude of past changes, using sensitivity tests to determine dependence of the
155 reconstructions on initial assumptions. The present study uses this approach for Lake
156 Mungo to reveal the major controls on otolith $\delta^{18}O$ in a quantitatively consistent manner.

157 In this study, we revisit the otolith oxygen isotope results from the Lake Mungo hearths
158 (Long et al., 2014). We develop a box model for lake filling and drying based on the
159 dimensions of the Willandra Lakes, modern evaporation rates for the region, and mass
160 balance principles including the Craig-Gordon (1965) model for oxygen isotope
161 fractionation during evaporation. This model is used to investigate how the oxygen
162 isotopes of Lake Mungo would have changed given Bowler's 'easy prey hypothesis'
163 (Bowler, 1998). In this hypothesis the Willandra Lakes episodically filled by flood events,
164 followed by evaporation-driven isotopes of Lake Mungo from the other lakes in the
165 system, which eventually culminated in desiccation of Lake Mungo.

166

167

METHODS

Site Description

Lake Mungo is one of 13 major (currently dry) palaeo-lakes that makes up the Willandra Lakes system. The Willandra Lakes existed intermittently in cycles of wet and dry conditions throughout the Quaternary, until they dried out completely at around 14.5 ka (Bowler, 1998; Bowler et al., 2012; Fitzsimmons et al., 2014). This series of basins is situated in arid New South Wales, Australia. Based on data from Pooncarie (Mulurulu station), 46 km north of Mungo, the average annual rainfall is 281 mm, lowest annual total 58 mm and highest is 803 mm, based on 135 years of data from 1882 to 2017 (BOM, 2020a). The mean annual evaporation rate for the region is 2000 mm/yr based on at least 10 years of records from 1975 to 2005 (BOM, 2020b). Seasonal evaporation rates range from 200 mm in Southern Hemisphere Winter (June, July, August) to 900 mm in Southern Hemisphere Summer (December, January, February) (BOM, 2020b). The area was inscribed on the World Heritage list in 1981 as a site of national and international significance for its testament to both the cultural history of Aboriginal people, and record of climatic and environmental changes throughout the Quaternary (Bowler et al., 1970; Bowler, 1998; Fitzsimmons et al., 2014; Stern, 2015).

A key feature of the Willandra Lakes is the sand/clay dunes (lunettes) that have built up on the windward side of each basin. Based on the topography of the lake system and the sedimentary characteristics of the lunettes, it is inferred that these lakes were once connected, forming an overflow outlet for the Lachlan River (Bowler et al., 1970, 1976). They were filled by large pulses of water that flowed from the Southern Tablelands of the Great Dividing Range down the Lachlan River into the Willandra Creek (Bowler et al.,

1976; Bowler, 1998; Kemp and Rhodes, 2010). This water sequentially filled Lake Mulurulu, and then Lakes Garnpung and Leaghur (Fig. 1). Lake Leaghur appears to have had two outflow points. The first is an overflow into Lake Mungo, the terminal lake in the system, via a shallow sill that separates the two lake basins. The second outflow is via the Willandra Creek and then continues past Lake Mungo to feed into the Outer Arumpo and Chibnalwood lakes, before eventually reaching the Prungle and Benenong Lakes further to the south (Magee, 1991; Barrows et al., 2020; Jankowski et al., 2020).

Study Species

The main fish species found in hearth sites at Lake Mungo is the golden perch (*Macquaria ambigua*, Richardson 1845). The golden perch is a long-lived species that is today found throughout the Murray Darling Basin, including the Lachlan River, preferring these predominately lowland, warmer, turbid, slow flowing rivers (Lintermans, 2007). These fish can tolerate a wide range of salinities (0–33 ppt) and temperatures (4–37°C), and both juveniles and sub-adults can even survive in seawater (Langdon, 1987). In modern systems, golden perch do not naturally congregate near the shoreline of lakes. Instead, they inhabit deep pools (~3 – 8 m) with woody debris, undercut banks, or rocky ledges (Cadwallader, 1979; Cadwallader and Backhouse, 1983; Battaglene and Prokop, 1987), and are usually fished using rods from small boats. Juvenile fish feed on aquatic insect larvae and microcrustaceans, while adults eat mainly shrimp, yabbies, small fish, and benthic aquatic insect larvae (Lintermans, 2007). Successful spawning and recruitment of golden perch typically requires elevated water temperatures and flooding (Humphries et al., 1999; Mallen-Cooper and Stuart, 2003; Ye et al., 2008; King et al., 2009). The otoliths of golden perch, like those of many other species, grow continuously and deposit

214 annual marks (light and dark bands) that, when viewed in thin section, have been
215 validated for ageing fish up to 22 years (Anderson et al., 1992; Stuart, 2006).

216 **Constructing the steady state model**

217 *Data sources*

218 This study focuses on comparing model results with oxygen isotope measurements from
219 three otoliths collected from a single hearth (#926) by the MAP in 2009. The fish otolith
220 oxygen isotope analysis was previously conducted and published as part of Long et al.
221 (2014). The otoliths of hearth 926 recorded a $\delta^{18}O$ increase of 7‰ over 6 years (#926-4),
222 9‰ over 8.5 years (#926-3) and 15‰ over 10 years (#926-1) (Fig. 2, adapted from Long
223 et al. (2014)).

224 A simple steady-state model was constructed to examine the influence of the hydraulic
225 controls on lake water $\delta^{18}O$ within the main Willandra Lakes, with emphasis on Lake
226 Mungo. The hydrological setting of Lake Mungo, and the Willandra Lakes system more
227 broadly, affects water $\delta^{18}O$ which, in turn, is recorded within the $\delta^{18}O$ of the preserved
228 otoliths. The isotopic starting point for the model is based on river records from the nearby
229 Barwon-Darling river system (Hughes et al., 2012).

230 *Establishing lake volumes and surface areas*

231 To construct the model, maximum water level, surface area and volumes were calculated
232 for each lake. Initially, the maximum water levels in each of the four modelled lake basins
233 were established using a digital elevation model (DEM) from the scanning radar
234 topography mission (SRTM), provided by Geoscience Australia. Here, the maximum
235 water level was controlled by the height of the outlet channel connecting each basin to

236 the next in the chain (Bowler et al., 2012). Using the DEM, the maximum lake level was
237 defined as the highest, closed 1 m contour line that resulted in separate lake basins. Next,
238 surface areas and volumes were determined by, first, excluding all contours that fell
239 outside of the highest closed 1m contour line in each lake. Surface area was then
240 calculated as the number of pixels within this contour, where each pixel represents a
241 known unit area. To determine lake volume, the surface area was calculated by identifying
242 pixels in 10 cm depth intervals from the base of the lake to the highest closed 1 m contour
243 line and integrating the series to estimate the volume at each respective 10 cm height.

244 *Establishing mass balance conditions for the model*

245 The starting point for the model is that all lakes are full; effectively, this hypothetically
246 represents the aftermath of a large flood event, as per the Bowler (1998) hypothesis. The
247 conditions required to maintain maximum lake levels are defined by water fluxes,
248 specifically: 1) the rate of evaporation from each lake's surface, 2) the extra water that is
249 needed to push water from one lake to the next, and 3) the amount of water needed to
250 maintain the height of the next lake in the sequence. For example, for the water height of
251 Lake Mungo to be maintained in a steady state, it needs to receive from Lake Leaghur as
252 much water as it is losing via evaporation. For Lake Leaghur to remain full it needs to
253 receive as much water as it loses through evaporation as well as loss to Lake Mungo,
254 where the latter is equivalent to the amount Lake Mungo loses via evaporation. Thus, the
255 basic relationship between water fluxes representing the inflow, evaporation and outflow
256 required to maintain lakes in mass balance is given by:

257 $$F_w = F_E + F_{out} \quad (1)$$

Where F_w is the water flux entering the lakes, F_E is the flux of water lost to evaporation and F_{out} is the water flux needed to maintain the heights of the lakes lower in the sequence. When $F_w = F_E + F_{out}$ then the lake level is stable because loss via evaporation is compensated exactly by inflowing water. When $F_w < F_E$ lake level will fall until empty because evaporation dominates. When $F_w > F_E$ inflowing water dominates over evaporation, the lake level will rise until full and then overflow (i.e., F_{out} becomes > 0). Similar expressions of these water fluxes for a chain or string of lakes are considered in Gibson and Reid (2014) and Gat and Bowser (1991).

The volume of water lost to evaporation from the first lake in the system is given by its surface area (SA) multiplied by the evaporation rate. The amount of outflow required is SA multiplied by the evaporation rate for each lake further down the system (see Fig. 3).

The water flux entering the Willandra Lakes system that is required to keep the water levels at a constant height can be expressed as:

$$F_w = SA_1E + SA_2E + SA_3E + SA_4E. \quad (2)$$

Where $\underline{F_w}$ is water flux entering the system, SA_1, SA_2… are the surface areas of the lakes from top to bottom of the Willandra sequence, and E is the evaporation rate for the region. If no water flows out of Lake Mungo, then to maintain stable lake levels throughout the model system the outflow for the top lake in the sequence must be equal to the sum of the surface area multiplied by the evaporation rate for each lake further down in the sequence or:

$$F_{out} = SA_2E + SA_3E + SA_4E \quad (3)$$

279 This gives us the amount of water needed to maintain all the lakes at mass balance after
280 an initial filling event. Now that we have established the model for maintaining water mass
281 balance, we turn to establishing the isotopic equilibrium conditions.

282 *Establishing isotopic equilibrium in the model*

283 Several variables affect the $\delta^{18}O$ of water bodies. In the model presented here, we take
284 into account the following variables: surface area and volume of the lakes, the regional
285 evaporation rates (annual, winter, and summer), equilibrium and kinetic effects on the
286 fractionation of water oxygen isotopes during evaporation, and the connections between
287 the lakes. Given the shallowness of the lakes (max. depth ~7-8m), their large surface
288 area, (Lake Mungo was ~140 km^2 when full; Barrows et al., 2020) to volume ratios and,
289 high wind speeds of the region (Mildura airport mean monthly wind speed between 9 and
290 20 km/hr, (BOM, 2020c)), the lakes are assumed to be well mixed. No direct lake-water
291 oxygen isotope measurements are available because the modern lake system is dry and
292 has not seen substantial water levels for the past ~16,000 years (Fitzsimmons et al.,
293 2014). Therefore, the isotopic starting point for the model is estimated based on $\delta^{18}O$
294 records from the nearby Barwon-Darling River as outlined in detail below (Hughes et al.,
295 2012). The following variables are not considered in the model as there are no robust
296 data available for this site at around 20,000 years ago: humidity, temperature,
297 groundwater input/output, and salinity.

298 It should be noted that, although the water $\delta^{18}O$ value used as a starting point for the
299 model influences the final equilibrium $\delta^{18}O$ value, it does not influence the rate or degree
300 of change over time. The rate and degree of change in water $\delta^{18}O$ over time is what we
301 are interested in for this study. We chose, therefore, to use a water $\delta^{18}O$ starting point of

-8‰ based on studies of water $\delta^{18}O$ in the nearby Barwon-Darling River (Meredith et al., 2009; Hughes et al., 2012). During high flow events, like those that once filled the Willandra Lakes, ephemeral tributaries of the Barwon-Darling River contribute ^{18}O-depleted water to the system. For example, Hughes et al., (2012) found that Darling River water at Bourke during the January 2004 high-flow event had a $\delta^{18}O$ of -8.32‰ relative to -3.23‰ in water measured upstream at Brewarrina. Fluvial input near Bourke of ^{18}O-depleted water from the Culgoa River, a normally dry tributary, caused the ~5‰ decrease in water $\delta^{18}O$ (Hughes et al., 2012). We assume for the Willandra Lakes model, that a large-scale flood event filled the lakes over a period of days, resulting from intense rainfall event(s). The isotopic composition of the source water in such a scenario is likely to be lighter (depleted in ^{18}O) than the composition of mean rainfall for the local or source region.

Using a -8‰ starting water $\delta^{18}O$ value, the equation for the isotopic steady state is given by:

$$F_{in}\,\Delta t\delta_P = F_E\Delta t(\delta_L - x) + F_{out}\Delta t\delta_L \quad (4)$$

Where δ_p is the isotopic composition of precipitation or water entering the lakes, δ_L is the isotopic composition of the lake water, ("$\delta_L - x$" gives the fractionation-related reduction in $\delta^{18}O$ relative to the source liquid. At a typical ambient temperature of 15-20°C, equilibrium fractionation results in approximately $\boldsymbol{x}$ = 10 (Gonfiantini, 1986; Froehlich et al., 2005; Rohling, 2016). In natural arid environments, this liquid-vapour offset can range from ~ 6‰ to 13‰, as measured respectively in evaporating water pans in arid Australia (Skrzypek et al., 2015; Gonfiantini et al., 2018) and the ephemeral Lake Gara Niba, Algerian Sahara, Northern Africa (Gonfiantini et al., 2018). Δt is the time step used in the

model when calculating how the system evolves through time. In the model, evaporation causes, the surface layer of each lake to become enriched in ^{18}O and the isotopically heavier surface water is then instantaneously mixed through the rest of the water column, before being passed on to the next lake in the sequence. Correspondingly, the first lake in the sequence was replenished with -8‰ water.

Running the steady state model – scenarios

The first phase of the steady state model involved setting up a series of connected boxes with the same dimensions as the Willandra Lakes basins and filling these instantly with water of $\delta^{18}O$ equal to -8‰, simulating a massive flood event into the dry basins. The lake water was then maintained at mass balance (inflow = outflow + evaporation), while the water $\delta^{18}O$ was allowed to adjust with evaporation and inflow according to equation 4. This was maintained for 20 years. Then we used the $\delta^{18}O$ value of water in Lake Mungo at the end of 20 years as the starting point for second phase of the model when we cut off inflow to Lake Mungo and allowed the water to evaporate.

We tested five different versions of the steady state model and the parameters of these are summarised in Table 1. In scenarios A, B and C we set F_E to the annual average evaporation rate for the region, 2000 mm/yr (BOM, 2020b), but in scenario B and C we changed the degree of evaporative fractionation in equation 4 from x = 10 (equilibrium) to x = 6 and x = 14 respectively, as a sensitivity test for changes in fractionation due to kinetic effects in natural arid environments (Skrzypek et al., 2015; Gonfiantini et al., 2018). In scenarios D and E we changed F_E from the modern annual average evaporation rate for the region (2000 mm/yr) to the Winter (800 mm/yr) and then Summer (3600 mm/yr)

evaporation rate, respectively (BOM, 2020b). This provides sensitivity tests with respect to the model's response to different evaporation rates.

RESULTS

Lake volume and surface area

The surface areas and volumes of Lake Mungo are shown as functions of water level in Figure 4. We find negligible changes in lake volume between 1 and 2 m water depths and a near linear increase in volume from 2 m to 7.5 m water depth to a maximum volume of ~5.5 x $10^8 m^3$. Surface area shows no appreciable increase until ~1.5 m water depth, before increasing rapidly to ~1x$10^8 m^2$ at 4 m water depth, and then remaining relatively stable until the maximum water depth is achieved.

Mass balance modelling

The results of the mass balance portion of the model, before the dashed line in Figure 5, show that the modelled water $\delta^{18}O$ of each lake basin increases as a function of both time and distance down the system. At Mulurulu, the first lake in the sequence, the modelled $\delta^{18}O$ of the lake water remains close to the -8‰ isotopic composition of the inflow in all four scenarios, only increasing by 1 to 2‰ over the 20-year period (Fig. 5). In contrast, the modelled water $\delta^{18}O$ values at Lake Mungo, the terminal lake in the sequence, increase rapidly before beginning to plateau.

Scenario A - evaporation set to 2000 mm/yr, equilibrium scenario, $x = 10$

In scenario A, F_E = 2000mm/yr and x = 10, the modelled $\delta^{18}O$ of water in Lake Mungo increased by ~18‰ in five years and eventually levels off at around 10 years at a value of 14‰ (total change of 22‰) which is maintained until the first part of the model ends at

20 years (Fig. 5A). The end value of 14‰ is used as the start of the second part of the model, when inflow to Lake Mungo is ceased the water is left to evaporate until the lake is essentially dry (10 cm depth). Following the cessation of inflow, the modelled water $\delta^{18}O$ for Lake Mungo increases by 16‰ in 2 years and continues to increase rapidly to beyond the limits of the graph.

Scenario B - evaporation set to 2000 mm/yr, x = 6

In scenario B, also with F_E = 2000 mm/yr, use x = 6 to allow for evaporation under reduced fractionation compared to equilibrium resulted in a lesser increase in the modelled Lake Mungo water $\delta^{18}O$; namely 11‰ in five years flattening at around 15 years to a value of 5.5‰ (total change of 13.5‰), which is maintained until the first part of the model ends at 20 years (Fig. 5B). In the second part of the model, when inflow to Lake Mungo ceases, the modelled water $\delta^{18}O$ increases by 10.5‰ in 2 years and continues to increase rapidly to beyond the limits of the graph.

Scenario C – evaporation set to 2000 mm/yr, x = 14

In scenario C, also with F_E = 2000 mm/yr, use x = 14 to allow for substantial kinetic fractionation effects resulted in a greater increase in the modelled Lake Mungo water $\delta^{18}O$; namely 25‰ in five years flattening within 12 years to a value of 23‰ (total change of 31‰), which is maintained until the first part of the model ends at 20 years (Fig. 5C). In the second part of the model, when inflow to Lake Mungo ceases, the modelled water $\delta^{18}O$ increases by 11‰ in 2 years and continues to increase rapidly to beyond the limits of the graph.

Scenario D - evaporation set to 800 mm/yr, equilibrium scenario, x = 10

391 Assuming that the modern Winter evaporation rate applies year-round, to define a
392 sensitivity test with a low annual evaporation-rate (scenario D), causes the lake water
393 $\delta^{18}O$ to increase more slowly towards isotopic equilibrium. At Lake Mungo, the water $\delta^{18}O$
394 increased by ~9‰ in the first five years of mass balance conditions, reaching ~13‰ at 20
395 years (total change of 21‰). In the second phase, when inflow into Lake Mungo is cut off
396 the modelled water $\delta^{18}O$ values increase by 5‰ in the first year and 18‰ over 5 years
397 (Fig. 5D).

398 *Scenario E - evaporation set to 3600 mm/yr, equilibrium scenario,* $x = 10$

399 Assuming that the modern Summer evaporation rate applies year-round, to define a
400 sensitivity test with a high annual evaporation-rate (scenario E) resulted in a faster
401 increase in water $\delta^{18}O$ during phase 1, with Lake Mungo water $\delta^{18}O$ increasing by 22‰
402 in the first 5 years, culminating in a $\delta^{18}O$ of about 14‰ after 20 years (Fig. 5E). When
403 inflow is cut off to Lake Mungo, in the second phase, the modelled water $\delta^{18}O$ values
404 increase especially sharply by 14‰ in the first year and >60‰ over 2 years.

405 **DISCUSSION**

406 Under water mass balance conditions (inflow = evaporation + outflow) the water $\delta^{18}Os$
407 will eventually approach isotopic equilibrium, a point at which there is no measurable
408 change in the isotopic composition of the water, we will refer to this point as “isotopic
409 balance”.

410 In the results for the mass balance portion of the model, before the dashed line in
411 Figure 5, the $\delta^{18}Os$ of the different lakes progress along similar trends to different points
412 of isotopic balance. The modelled water $\delta^{18}O$ for Lake Mulurulu at the top of the sequence

413 remains fairly low and close to the -8‰ of incoming water in all scenarios. The lakes
414 further down the sequence (Leaghur, Garnpung and Mungo) reach successively higher
415 isotopic balance points than Lake Mulurulu. These results are a direct consequence of
416 evaporation and the connections between the lakes, with each lake passing on water that
417 is isotopically heavier (i.e. higher $\delta^{18}O$) than the water it received from the previous lake.
418 Ultimately, this causes lakes further from the primary water source to reach higher $\delta^{18}O$
419 levels than lakes closer to the source. These results further demonstrate the string-of-
420 lakes effect on water $\delta^{18}O$ discussed by Gat and Bowser (1991) and Gibson and Reid
421 (2014). If we had modelled water mass balance for Lake Mungo in isolation, then the
422 dependence of Lake Mungo water $\delta^{18}O$ on processes in the lakes higher in the system
423 would have been neglected.

424 **Comparison between the models and the otoliths**

425 The impact of removing inflow on the $\delta^{18}O$ of Lake Mungo water is shown after the dotted
426 line in Figure 5. This is the point at which we isolated Lake Mungo and allowed the water
427 to evaporate at the given rate until the lake is effectively dry (10 cm deep). Any fish that
428 were living in the lake during the full extent of this trend would have died and been
429 deposited on the lake floor. The fish otoliths that are the focus of this and the previous
430 study (Long et al., 2014) were all collected from hearth sites on the lakeshore, which
431 suggests that they did not die naturally in the lake but were collected and eaten. The
432 original interpretation of the increasing trends in the hearth otolith $\delta^{18}O$ records proposed
433 that they resulted from water changes associated with progressive drying out, and
434 lowering of lake levels (Long et al., 2014). In all scenarios tested here, the change in
435 water $\delta^{18}O$ values when Lake Mungo is cut-off and evaporating is much more rapid and

436 of much greater amplitude than the changes recorded in the hearth otoliths. Within 5
437 years of inflow cut-off, the $\delta^{18}O$ in all scenarios increased by >18‰, in scenario E this
438 even happens within 2 years (Fig. 5E). When we compare this to the maximum change
439 recorded in the hearth otolith $\delta^{18}O$ records, 15‰ increase over 10 years
440 (926- 1, Fig. 2), it becomes apparent that it is improbable that these fish were collected
441 from a lake evaporating to dryness.

442 The results of this study show that under mass balance conditions, represented before
443 the dotted line in Figure 5, the modelled water $\delta^{18}O$ of Lake Mungo increases to a point
444 and then flattens. This happens in all five scenarios. These trends closely follow those
445 observed in the hearth otoliths, in particular Otolith #926-1, which shows a sharper
446 increase in early life and a flatter trend in later life (Fig. 2). The total increase in hearth
447 otolith $\delta^{18}O$ is in the order of 10-15‰ over 10 years (Otolith #926-1, Fig. 2). This rate of
448 change is most similar to the results for Winter evaporation rate scenario D, where the
449 increase in modelled water $\delta^{18}O$ for Lake Mungo under mass balance conditions is 16‰
450 in 10 years (Fig. 5D).

451 Although the increasing trend in the hearth otoliths from Lake Mungo was initially
452 interpreted (Long et al., 2014) in a qualitative manner in terms of inflow cut-off and
453 subsequent lake desiccation, supporting the “easy prey” hypothesis (Bowler, 1998). our
454 model-based quantitative assessment indicates that, this can no longer be supported.
455 Instead, we find that hearth otolith $\delta^{18}O$ records are more representative of a recently
456 flooded lake that is maintained in mass balance under relatively low evaporation
457 conditions (<800 mm/yr). That is, the otolith records are registering a change in oxygen
458 isotopes with evaporation, but not a change in lake volume and, thus, level.

Given the similarities between the winter mass balance model results (scenario D) and the otolith observations, we infer that the golden perch living in Lake Mungo between ~19,000 and 19,500 years ago were living in a mass balanced system with steady lake level, which gradually developed toward isotopic mass balance (equilibrium). We contend that it is highly unlikely that Lake Mungo evaporated to dryness during the period represented by the fish bone hearths. The very rapid trend in water $\delta^{18}O$ that would characterise evaporating lake conditions is not reflected in the hearth otolith data. This re-interpretation of the otolith records fits well with recent work at Lake Mungo which suggests increased availability of surface water during the LGM as a result of lower evaporation rates and increased runoff (Barrows et al., 2020).

Fish otolith $\delta^{18}O$ and lake level modelling compared to sedimentary records

Sedimentary archives provide a broad range of information concerning lake hydrology, and Optically Stimulated Luminescence (OSL) dating has proven invaluable for putting this information into a chronological sequence (Fitzsimmons et al., 2014; Barrows et al., 2020; Jankowski et al., 2020). The difficulty comes with matching these records with Aboriginal presence on the lakeshore. Otoliths and shells from hearth sites and middens are already being used to radiocarbon date hearth sites on the lakeshore and link this to the sediments in which they lie (Stern, 2015) but there is further value in these otoliths and shells. The sub annual records in otoliths can add detail to the local lake level history, experienced by people in the past. When coupled with mass balance modelling, as shown here, we can start to rule out some scenarios for lake conditions and add weight to others.

Otolith – diagenetic, cooking and trash disposal effects

Modern golden perch fish otoliths are typically composed entirely of aragonite. Post diagenetic effects like heating can cause the aragonite to recrystallize into the more stable polymorph calcite. In archaeological otolith samples the absence of calcite is usually a good indication that an otolith has not been affected by chemical alteration. Two of the ancient hearth otoliths were tested using XRD and neither were found to contain measurable calcite (Long et al., 2014). This provides some assurance that recrystallization has not occurred.

In regards to the effect of cooking on fish otolith oxygen isotopes, Disspain et al., (2016) applied a range of different cooking methods to black bream and found that otoliths that had been heated had lower mean $\delta^{18}O$ compared to the control group. Differences in $\delta^{18}O$ between heat treated otoliths and the control group ranged from -1.09 to -1.47‰ except for the otoliths that were burnt. Burnt otoliths were visibly blackened with a chalky texture and these had $\delta^{18}O$ values 4.37‰ lower that the control. This is similar to the results of cooking experiments conducted by Andrus and Crowe (2002) who found that the $\delta^{18}O$ of burnt Atlantic Croaker (*Micropogonius undulatus*) and catfish (*Bagre marinus*) otoliths were 1.8 to 3.1 ‰ lower than the control sample. The study by Long et al.,(2014) avoided any otoliths that showed signs of burning (blackened surface) but it is possible that they experienced heating. If we take into account the possibility that heating affected hearth otolith $\delta^{18}O$ values then they should all be 1-2‰ higher, as heating would have caused the original $\delta^{18}O$ value to decrease. There would be no change in the slope of the observed trend and so this does not increase support for an evaporating lake scenario.

Evaporation rate, equilibrium and kinetic fractionation

The annual average evaporation rate during the Last Glacial Maximum (LGM) is unknown. Likewise, the effect of ambient conditions on the isotopic fractionation of water during evaporation is unknown for the LGM. Therefore, we tested multiple evaporation rates and both equilibrium and kinetic values for x in equation 4 to determine what effect these have on the modelled water $\delta^{18}O$. The results showed that the evaporation rate affects how quickly the water $\delta^{18}O$ increases towards isotopic balance, while the fractionation rate controls how high that isotopic balance point is. All the scenarios with the same x value in equation 4 will eventually reach the same isotopic balance point but the time this takes differs. In the Summer scenario (Fig. 5E), which had the highest evaporation rate, the increase in modelled water $\delta^{18}O$ for Lake Mungo occurs quite quickly, reaching isotopic balance within 10 years. In contrast, the Winter evaporation scenario (Fig. 5D) with the lowest evaporation rate yields a the modelled water $\delta^{18}O$ curve for Lake Mungo that is flatter and only reaches 13‰ within the 20 years of the model. If we extended the time frame for this portion of the model, then it would eventually flatten out at ~14‰. By changing the value for x from "10" in the scenario A to "14" in the scenario C (Fig. 5C), we increase the isotopic balance point from ~14‰ to ~23‰. By reducing the value for x to "6" in scenario B (Fig. 5B) we reduce the isotopic balance point to ~5.5‰. Even with this reduced value of x the change in the water $\delta^{18}O$ of Lake Mungo, 11‰ in 5 years, is still greater and faster than the change observed in the otoliths, 15‰ in 10 years. Regardless of there being only equilibrium (x = 10) or equilibrium+kinetic ($x = 10 \pm 4$, based on water bodies evaporating in similarly arid environments (Gonfiantini et al., 2018)) fractionation during evaporation, the change in water $\delta^{18}O$ when Lake Mungo is cut off and left to evaporate is still much more pronounced than that seen

526 in the otoliths. For the model presented here, the only way that the trend can be flattened
527 out to more closely match the otoliths is by changing the evaporation rate.

528 **Model limitations**

529 In all models there are limitations around what can and cannot be inferred (Box, 1976).
530 The model created here is not a true-to-life simulation of climate and lake conditions at
531 the Willandra Lakes during the LGM. Instead it is a simplified model that only considers
532 the amount of water needed to fill the lakes, the annual evaporation rate and basic isotopic
533 theory for fractionation of water during evaporation. There are usually sub-annual to
534 decadal changes in temperature, humidity, water input, evaporation rate and other factors
535 that are simply unknown for this time period at the scale needed to compare to the life of
536 a fish.

537 The mass balance models presented here do not include contributions from groundwater.
538 It has been suggested by Bowler et al., (2012) that during the final drying of the lower
539 lakes in the system, influx of seasonal high salinity groundwater would have produced
540 clay dunes with a high gypsum content. So far, the only lake where high gypsum clays
541 are observed on the lunettes is at Chibnalwood/Arumpo which is below Lake Leaghur in
542 the sequence and not directly connected to Lake Mungo. These lakes are not considered
543 in the present scenario and there is no evidence of a gypsum clay phase at Lake Mungo
544 (Bowler et al., 2012).

545 In the nearby Darling River groundwater exchanges were found to increase the river water
546 Cl- content (increasing the salinity) but the depletion in the stable isotope values by mixing
547 with depleted groundwater was found to be overwhelmed by evaporative enrichment
548 (Meredith et al., 2009). Those authors could only identify the impact of groundwater input

549 on the oxygen isotopes by sampling at a high spatial and temporal resolution within a
550 short distance of the river. Similar conclusions were reached by Simpson and Herczeg
551 (1991), who observed that groundwater influx had a major impact on salinity levels when
552 Darling River waters were low, whereas the impact on the isotopes of the river water was
553 minor. In the present study we are comparing our model outputs to the otolith records,
554 which at best contain an annual average trend and are unlikely to pick up the short-term
555 influence of groundwater isotopic input. We have therefore decided not to include this in
556 our model.

557 The salinity of water at the Willandra Lakes in the past is unknown but it is expected that
558 any salts accumulating in the upstream lakes would be flushed downstream during flood
559 events (Bowler et al., 2012). This would result in increased salinity during evaporation
560 and higher salinity at lakes lower in the chain. In marine or near-marine salinities,
561 evaporation can result in a reversal in the enrichment process of the oxygen isotopes
562 during evaporation (Gonfiantini, 1986; Gat, 1995). There is no reversing trend evident in
563 the otolith oxygen isotope values and so it is unlikely that salinity was high enough to
564 cause this effect, thus it is not considered in the model scenarios.

565 If humidity were included in the model, we would likely find a change in the evaporative
566 slope. Heavy isotope enrichment is considerable when humidity is low but the effect is
567 reduced when humidity is higher (Gat and Bowser, 1991). Humidity also has a role to play
568 in limiting the isotopic enrichment of the lake water. At humidity 0.75 (75%) the limiting
569 value for a lake of 0‰ is +8‰. For humidity 0.50 (50%) the same lake has a limiting value
570 of around 24‰ and at humidity's of 25% the limit is >40‰. Again there are no records for

humidity at Lake Mungo during the LGM but a follow up mass balance model could test different scenarios to see what effect this has on the oxygen isotope trends.

Conclusions

Our reappraisal of the $\delta^{18}O$ records preserved in golden perch (*Macquaria ambigua*) otoliths from archaeological contexts at the Lake Mungo World Heritage site indicates that the fish did not die in a lake that was cut off from the river system and evaporating to dryness. Our calculations instead suggest that the annual evaporation rate for the region was lower than it is today and that lake levels were more-or-less stable; i.e., the fish were living in a mass-balanced system and the otolith $\delta^{18}O$ increase resulted from gradual development of the ambient water toward isotopic balance. The trend in otolith $\delta^{18}O$ values was most similar to those of the water when the lakes were all full and evaporative rates were set to 800 mm/yr. Our results also have implications for interpretation of Aboriginal fishing practices. The hypothesis that people were taking advantage of sluggish oxygen-starved golden perch, in a drying-out lake system does not seem to be supported. Hence, consideration needs to be given to other fishing techniques and, thus, the role of fish in the diet. Further development of the implications will require both further oxygen isotope records across otolith (or shell) age increments from the Willandra Lakes, and further refinement of the modelling to account for variation in environmental factors such as humidity, temperature, precipitation, and groundwater processes.

Acknowledgements

We would like to thank Nicola Stern and Nathan Jankowski for providing comments on the sections related to the archaeology and geology of Lake Mungo and the Willandra Lakes and Matthew Jones for providing comments on the modelling aspects of this study.

We would also like to acknowledge and thank the Traditional Owners of the land on which this work was conducted; the Elders of the Three Traditional Tribal Groups from the Willandra Lakes region, the Paakantyi/Barkindji, the Mutthi Mutthi and the Ngiyampaa for their interest in and support of this work. This research was supported in part by ARC DP150100487 and ARC DP1092966.

Declarations of interest: none

References:

Allen, H., Holdaway, S., 2009. The archaeology of Mungo and the Willandra Lakes: looking back, looking forward. Archaeol. Oceania 44, 96–106.

Anderson, J.R., Morison, A.K., Ray, D.J., 1992. Validation of the Use of Thin-sectioned Otoliths for Determining the Age and Growth of Golden Perch, Macquaria ambigua (Perciformes: Percichthyidae), in the Lower Murray-Darling Basin, Australia. Australian Journal of Marine and Freshwater Resources 43, 1103–1128.

Andrus, C.F.T., Crowe, D.E., 2002. Alteration of Otolith Aragonite: Effects of Prehistoric Cooking Methods on Otolith Chemistry. Journal of Archaeological Science 29, 291–299. https://doi.org/10.1006/jasc.2001.0694

Andrus, C.F.T., Crowe, D.E., Sandweiss, D.H., Reitz, E.J., Romanek, C.S., 2002. Otolith delta 18O record of mid-Holocene sea surface temperatures in Peru. Science (New York, N.Y.) 295, 1508–11. https://doi.org/10.1126/science.1062004

Barrows, T.T., Fitzsimmons, K.E., Mills, S.C., Tumney, J., Pappin, D., Stern, N., 2020. Late Pleistocene lake level history of Lake Mungo, Australia. Quaternary Science Reviews 238, 106338. https://doi.org/10.1016/j.quascirev.2020.106338

616 Barrows, T.T., Juggins, S., De Deckker, P., Calvo, E., Pelejero, C., 2007. Long-term sea
617 surface temperature and climate change in the Australian-New Zealand region.
618 Paleoceanography 22. https://doi.org/10.1029/2006PA001328

619 Battaglene, S., Prokop, F., 1987. Golden perch, Agfacts F3.2.2. Grafton, Austrlia.

620 BOM, 2020a. Monthly Rainfall Data, Pooncarie (Mulurulu Station) [WWW Document].
621 URL
622 http://www.bom.gov.au/jsp/ncc/cdio/weatherData/av?p_nccObsCode=139&p_displ
623 ay_type=dataFile&p_startYear=&p_c=&p_stn_num=047024 (accessed 7.16.20).

624 BOM, 2020b. Average annual, monthly and seasonal evaporation [WWW Document].
625 URL http://www.bom.gov.au/jsp/ncc/climate_averages/evaporation/index.jsp
626 (accessed 11.7.20).

627 BOM, 2020c. Monthly Climate Statistics, MILDURA AIRPORT, [WWW Document]. URL
628 http://www.bom.gov.au/climate/averages/tables/cw_076031.shtml (accessed
629 7.22.20).

630 Bowler, J.M., 1998. Willandra Lakes Revisited: Environmental Framework for Human
631 Occupation. Archaeology in Oceania 33, 120–155. https://doi.org/10.1002/j.1834-
632 4453.1998.tb00414.x

633 Bowler, J.M., Gillespie, R., Johnston, H., Boljkovac, K., Bolijkovac, K., 2012. Wind v
634 water: Glacial maximum records from the Willandra Lakes. Peopled Landscapes:
635 Archaeological and Biogeographic Approaches to Landscapesl 34, 271–296.

636 Bowler, J.M., H. Johnston, J. M. Olley, J. R. Prescott, R. G. Roberts, W. Shawcross,
637 Spooner, N.A., 2003. New Ages for human occupation and climatic change at Lake

638 Mungo, Australia. Nature 421, 837–840.

639 Bowler, J.M., Hope, G.S., Jennings, J.N., Singh, G., Walker, D., 1976. Late Quaternary
640 climates of Australia and New Guinea. Quaternary Research 6, 359–394.
641 https://doi.org/10.1016/0033-5894(67)90003-8

642 Bowler, J.M., Jones, R., Allen, H., Thorne, A.G., 1970. Pleistocene Human Remains from
643 Australia: A Living Site and Human Cremation from Lake Mungo, Western New
644 South Wales. World Archaeology 2, 39–60.

645 Box, G.E.P., 1976. Science and statistics. Journal of the American Statistical Association
646 71, 791–799. https://doi.org/10.1080/01621459.1976.10480949

647 Cadwallader, P.L., 1979. Distribution of native and introduced fish in the Seven Creeks
648 River system, Victoria. Australian Journal of Ecology 4, 361–385.

649 Cadwallader, P.L., Backhouse, G.N., 1983. A guide to the freshwater fish of Victoria.

650 Campana, S.E., 1999. Chemistry and composition of fish otoliths: pathways, mechanisms
651 and applications. Marine Ecology Progress Series 188, 263–297.

652 Craig, H., Gordon, L., 1965. Deuterium and oxygen 18 variations in the ocean and the
653 marine atmosphere, Stable Isotopes in Oceanographic Studies and
654 Paleotemperatures.

655 Craig, H., Gordon, L.I., Horibe, Y., 1963. Isotopic exchange effects in the evaporation of
656 water: 1. Low-temperature experimental results. Journal of Geophysical Research
657 68, 5079–5087. https://doi.org/10.1029/jz068i017p05079

658 Dinçer, T., 1968. The Use of Oxygen 18 and Deuterium Concentrations in the Water
659 Balance of Lakes. Water Resources Research 4, 1289–1306.

660 Disspain, M.C.F., Ulm, S., Izzo, C., Gillanders, B.M., 2016. Do fish remains provide
661 reliable palaeoenvironmental records? An examination of the effects of cooking on
662 the morphology and chemistry of fish otoliths, vertebrae and scales. Journal of
663 Archaeological Science 74, 45–59. https://doi.org/10.1016/J.JAS.2016.08.010

664 Dufour, E., Van Neer, W., Vermeersch, P.M., Patterson, W.P., 2018. Hydroclimatic
665 conditions and fishing practices at Late Paleolithic Makhadma 4 (Egypt) inferred from
666 stable isotope analysis of otoliths. Quaternary International 471, 190–202.
667 https://doi.org/10.1016/j.quaint.2017.09.026

668 Fitzsimmons, K., Stern, N., Murray-Wallace, C. V., 2014. Depositional history and
669 archaeology of the central Lake Mungo lunette, Willandra Lakes, southeast Australia.
670 Journal of Archaeological Science 41, 349–364.
671 https://doi.org/10.1016/j.jas.2013.08.004

672 Froehlich, K.F.O., Gonfiantini, R., Rozanski, K., 2005. Isotopes in Lake Studies: A
673 Historical Perspective, in: Isotopes in the Water Cycle. Springer-Verlag,
674 Berlin/Heidelberg, pp. 139–150. https://doi.org/10.1007/1-4020-3023-1_11

675 Gat, J.R., 1995. Stable Isotopes of Fresh and Saline Lakes. Physics and Chemistry of
676 Lakes 60, 139–163. https://doi.org/10.1016/0016-7037(96)83277-7

677 Gat, J.R., Bowser, C., 1991. The heavy isotope enrichment of water in coupled
678 evaporative systems. Stable Isotope Geochemistry: A Tribute to Samuel Epstein
679 Special Pu, 159–168.

680 Geffen, A.J., Høie, H., Folkvord, A., Hufthammer, A.K., Andersson, C., Ninnemann, U.,
681 Pedersen, R.B., Nedreaas, K., 2011. High-latitude climate variability and its effect on

682 fisheries resources as revealed by fossil cod otoliths. ICES Journal of Marine Science
683 68, 1081–1089.

684 Gibson, J.J., Birks, S.J., Yi, Y., 2016. Stable isotope mass balance of lakes: A
685 contemporary perspective. Quaternary Science Reviews 131, 316–328.
686 https://doi.org/10.1016/j.quascirev.2015.04.013

687 Gibson, J.J., Edwards, T.W.D., 2002. Regional water balance trends and evaporation-
688 transpiration partitioning from a stable isotope survey of lakes in northern Canada.
689 Glob. Biogeochem. Cycles 16, 1026.

690 Gibson, J.J., Edwards, T.W.D., Prowse, T.D., 1996. Development and validation of an
691 isotopic method for estimating lake evaporation. Hydrological processes 10, 1369–
692 1382.

693 Gibson, J.J., Reid, R., 2014. Water balance along a chain of tundra lakes: A 20-year
694 isotopic perspective. Journal of Hydrology 519, 2148–2164.
695 https://doi.org/10.1016/j.jhydrol.2014.10.011

696 Gonfiantini, R., 1986. Environmental isotopes in lake studies, in: Handbook of
697 Environmental Isotope Geochemistry. pp. 113–168.

698 Gonfiantini, R., Wassenaar, L.I., Araguas-Araguas, L., Aggarwal, P.K., 2018. A unified
699 Craig-Gordon isotope model of stable hydrogen and oxygen isotope fractionation
700 during fresh or saltwater evaporation. Geochimica et Cosmochimica Acta 235, 224–
701 236. https://doi.org/10.1016/j.gca.2018.05.020

702 Hesse, P.P., Magee, J.W., van der Kaars, S., 2004. Late Quaternary climates of the
703 Australian arid zone: a review. Quaternary International 118–119, 87–102.

https://doi.org/10.1016/s1040-6182(03)00132-0

Hughes, C.E., Stone, D.J.M., Gibson, J.J., Meredith, K.T., Sadek, M.A., Cendon, D.I., Hankin, S.I., Hollins, S.E., Morrison, T.N., 2012. Stable water isotope investigation of the Barwon-Darling River System, Australia, in: Monitoring Isotopes in Rivers : Creation of the Global Network of Isotopes in Rivers (GNIR). pp. 97–110.

Humphries, P., King, A., Koehn, J., 1999. Fish, flows and flood plains: links between freshwater fishes and their environment in the Murray-Darling River system, Australia. Environmental Biology of Fishes.

Jankowski, N.R., Stern, N., Lachlan, T.J., Jacobs, Z., 2020. A high-resolution late Quaternary depositional history and chronology for the southern portion of the Lake Mungo lunette, semi-arid Australia. Quaternary Science Reviews 233, 106224. https://doi.org/10.1016/j.quascirev.2020.106224

Jones, M.D., 2013. What do we mean by wet? Geoarchaeology and the reconstruction of water availability. Quaternary International 308–309, 76–79. https://doi.org/10.1016/j.quaint.2012.12.015

Jones, M.D., Cuthbert, M.O., Leng, M.J., McGowan, S., Mariethoz, G., Arrowsmith, C., Sloane, H.J., Humphrey, K.K., Cross, I., 2016. Comparisons of observed and modelled lake δ18O variability. Quaternary Science Reviews 131, 329–340. https://doi.org/10.1016/j.quascirev.2015.09.012

Jones, M.D., Leng, M.J., Roberts, C.N., Türkeş, M., Moyeed, R., 2005. A coupled calibration and modelling approach to the understanding of dry-land lake oxygen isotope records. Journal of Paleolimnology 34, 391–411.

https://doi.org/10.1007/s10933-005-6743-0

Kalish, J.M., 1991. Oxygen and carbon stable isotopes in the otoliths of wild and laboratory-reared Australian salmon (Arripis trutta). Marine Biology 47, 37–47.

Kemp, J., Rhodes, E.J., 2010. Episodic fluvial activity of inland rivers in southeastern Australia: Palaeochannel systems and terraces of the Lachlan River. Quaternary Science Reviews 29, 732–752. https://doi.org/10.1016/j.quascirev.2009.12.001

Kerr, L., Secor, D., Kraus, R., 2007. Stable isotope (δ13C and δ18O) and Sr/Ca composition of otoliths as proxies for environmental salinity experienced by an estuarine fish. Marine Ecology Progress Series 349, 245–253. https://doi.org/10.3354/meps07064

King, A.J., Tonkin, Z., Mahoney, J., 2009. Environmental flow enhances native fish spawning and recruitment in the Murray River, Australia. River Research and Applications 25, 1205–1218.

Lacey, J.H., Jones, M.D., 2018. Quantitative reconstruction of early Holocene and last glacial climate on the Balkan Peninsula using coupled hydrological and isotope mass balance modelling. Quaternary Science Reviews 202, 109–121. https://doi.org/10.1016/j.quascirev.2018.09.007

Langdon, J.S., 1987. Active osmoregulation in the Australian Bass, Macquaria novemaculeata(Steindachner), and the golden perch, Macquaria ambigua (Richardson) (Percichthyidae). Marine and Freshwater Research 38, 771–776. https://doi.org/http://dx.doi.org/10.1071/MF9870771

Leng, M.J., Lewis, J.P., 2014. Oxygen isotopes in Molluscan shell: Applications in

environmental archaeology. Environmental Archaeology 21, 295–306. https://doi.org/10.1179/1749631414y.0000000048

Leng, M.J., Marshall, J.D., 2004. Palaeoclimate interpretation of stable isotope data from lake sediment archives, in: Quaternary Science Reviews. pp. 811–831. https://doi.org/10.1016/j.quascirev.2003.06.012

Lintermans, M., 2007. Fishes of the Murray-Darling Basin: an introductory guide, MDBC Publication, Murray-Darling Basin Commission, Canberra, Australia.

Long, K., Stern, N., Williams, I.S., Kinsley, L., Wood, R., Sporcic, K., Smith, T., Fallon, S., Kokkonen, H., Moffat, I., Gr??n, R., 2014. Fish otolith geochemistry, environmental conditions and human occupation at Lake Mungo, Australia. Quaternary Science Reviews 88, 82–95.

Long, K., Wood, R., Williams, I.S., Kalish, J., Shawcross, W., Stern, N., Grün, R., 2018. Fish otolith microchemistry: Snapshots of lake conditions during early human occupation of Lake Mungo, Australia. Quaternary International 463, 29–43. https://doi.org/10.1016/j.quaint.2016.10.026

Macdonald, J.I., Crook, D.A., 2010. Variability in Sr: Ca and Ba: Ca ratios in water and fish otoliths across an estuarine salinity gradient. Marine Ecology Progress Series 413, 147–161.

Magee, J.W.W., 1991. Late Quaternary lacustrine , groundwater , aeolian and pedogenic gypsum in the Prungle Lakes , southeastern Australia. Palaeogeography, Palaeoclimatology, Palaeoecology 84, 3–42.

Mallen-Cooper, M., Stuart, I.G., 2003. Age, growth and non-flood recruitment of two

potamodromous fishes in a large semi-arid/temperate river system. River Research and Applications 19, 697–719. https://doi.org/10.1002/rra.714

Mannino, M.A., Thomas, K.D., Leng, M.J., Sloane, H.J., 2008. Shell growth and oxygen isotopes in the topshell Osilinus turbinatus: Resolving past inshore sea surface temperatures. Geo-Marine Letters 28, 309–325. https://doi.org/10.1007/s00367-008-0107-5

McTainsh, G.H., Lynch, A.W., 1996. Quantitative estimates of the effect of climate change on dust storm activity in Australia during the last glacial maximum. Geomorphology 17, 263–271. https://doi.org/10.1016/0169-555x(95)00106-f

Meredith, K.T., Hollins, S.E., Hughes, C.E., Cendón, D.I., Hankin, S., Stone, D.J.M., 2009. Temporal variation in stable isotopes (18O and 2H) and major ion concentrations within the Darling River between Bourke and Wilcannia due to variable flows, saline groundwater influx and evaporation. Journal of Hydrology 378, 313–324. https://doi.org/http://dx.doi.org/10.1016/j.jhydrol.2009.09.036

Olley, J.M., Roberts, R.G., Yoshida, H., Bowler, J.M., 2006. Single-grain optical dating of grave-infill associated with human burials at Lake Mungo, Australia. Quaternary Science Reviews 25, 2469–2474. https://doi.org/10.1016/j.quascirev.2005.07.022

Reeves, J.M., Barrows, T.T., Cohen, T.J., Kiem, A.S., Bostock, H.C., Fitzsimmons, K.E., Jansen, J.D., Kemp, J., Krause, C., Petherick, L., Phipps, S.J., 2013. Climate variability over the last 35,000 years recorded in marine and terrestrial archives in the Australian region: an OZ-INTIMATE compilation. Quaternary Science Reviews 74, 21–34. https://doi.org/10.1016/j.quascirev.2013.01.001

792 Rohling, E.J., 2016. Of lakes and fields: A framework for reconciling palaeoclimatic
793 drought inferences with archaeological impacts. Journal of Archaeological Science
794 73, 17–24. https://doi.org/10.1016/j.jas.2016.07.005

795 Simpson, H.J., Herczeg, A.L., 1991. Salinity and evaporation in the River Murray Basin,
796 Australia. Journal of Hydrology 124, 1–27. https://doi.org/10.1016/0022-
797 1694(91)90003-Z

798 Skrzypek, G., Mydłowski, A., Dogramaci, S., Hedley, P., Gibson, J.J., Grierson, P.F.,
799 2015. Estimation of evaporative loss based on the stable isotope composition of
800 water using Hydrocalculator. Journal of Hydrology 523, 781–789.
801 https://doi.org/10.1016/j.jhydrol.2015.02.010

802 Stern, N., 2015. 13 . The Archaeology of the Willandra Its empirical structure and narrative
803 potential, in: McGrath, A., Jebb, M.A. (Eds.), Long History, Deep Time: Deepening
804 Histories of Place. ANU Press, Canberra, pp. 221–240.

805 Stern, N., Tumney, J., Kajewski, P., 2013. Strategies for investigating human responses
806 to changes in landscape and climate at Lake Mungo in the Willandra Lakes,
807 southeast Australia, in: Frankel, D., Webb, J., Lawrence, S. (Eds.), Archaeology in
808 Technology and Environment. Routledge, London, pp. 31–50.

809 Stuart, I.G., 2006. Validation of Otoliths for Determining Age of Golden Perch, a Long-
810 Lived Freshwater Fish of Australia. North American Journal of Fisheries
811 Management 26, 52–55. https://doi.org/10.1577/M05-077.1

812 Washburn, E.W., Urey, H.C., 1932. Concentration of the H2 Isotope of Hydrogen by the
813 Fractional Electrolysis of Water, Proceedings of the National Academy of Sciences

814 of the United States of America. https://doi.org/10.1073/pnas.18.7.496

815 Weidman, C.R., Millner, R., 2000. High-resolution stable isotope records from North
816 Atlantic cod. Fisheries Research 46, 327–342. https://doi.org/10.1016/S0165-
817 7836(00)00157-0

818 Ye, Q., Cheshire, K., Fleer, D., Centre, S.A.A.S., 2008. Recruitment of golden perch and
819 selected large-bodied fish species following the weir pool manipulation in the River
820 Murray, South Australia.

821 Zimmerman, C.E., 2005. Relationship of otolith strontium-to-calcium ratios and salinity :
822 experimental validation for juvenile salmonids. Canadian Journal of Fisheries and
823 Aquatic Sciences 62, 88–97. https://doi.org/10.1139/F04-182

824

825 **Figures:**

826 Figure 1: Map of the northern part of the Willandra Lakes system showing the main lakes
827 used in the model, Mulurulu, Garnpung, Leaghur and Mungo, adapted from Bowler
828 (1998).

829 Figure 2: The oxygen isotope values plotted against otolith age lines as years before
830 death for each of the otoliths collected from hearth #926 (Long et al., 2014). Adult life is
831 on the left and juvenile stage is on the right.

832 Figure 3: Schematic representation of the water flux entering the Willandra Lakes as
833 expressed by Equations 1, 2 and 3. Note, the equation shown is for the specific case of
834 Lake Mulurulu and in the model is adjusted appropriately for each lake downstream.

835 Figure 4: Modelled change in Lake Mungo surface area and volume with depth.

Figure 5: Modelled output for change in the water $\delta^{18}O$ of the Willandra lakes when the lake levels are maintained in mass balance for 20 years (before the dashed vertical line), and then the changes in the water $\delta^{18}O$ of Lake Mungo when it is cut off from the rest of lakes and left to evaporate to dryness (10 cm depth) after those 20 years (after the dashed vertical line). Five different scenarios are shown: A) evaporation rate is set to 2000 mm/year and x is set to 10 in equation 4, B) evaporation rate is set to 2000 mm/yr and x is set to 6 in equation 4, C) evaporation rate is set to 2000 mm/yr and x is set to 14 in equation 4, D) evaporation rate is set to 800 mm/year x is set to 10 in equation 4, E) evaporation rate is set to 3600 mm/yr, x is set to 10 in equation 4.

Tables:

Table 1: Summary of the modelled scenarios for the Willandra Lakes, evaporation rates are based on historical records for the region from the Bureau of Meteorology (2020b), starting water values are estimated based on studies of nearby river systems (Hughes et al., 2012).

Matlab code

height2F

```
function [FIN,FE,FOUT,V]=height2F(H0,E)

load lake_splines

pp{1}.SA=Mulurulu.SA;
pp{2}.SA=Garnpung.SA;
pp{3}.SA=Leaghur.SA;
pp{4}.SA=Mungo.SA;
pp{5}.SA=Arumpo.SA;

%% add static head to lakes
```

```
z=1; %add 1 metre
for i=1:numel(pp)
xhat=pp{i}.SA.breaks;
yhat=ppval(pp{i}.SA,xhat);
dz=xhat(2)-xhat(1);
xhat0=[xhat,(xhat(end)+dz:dz:xhat(end)+z)];
dSA=ppval(fnder(pp{1}.SA),xhat(end));
yhat0=[yhat,yhat(end)+(dz:dz:z)*dSA];
pp{i}.SA=pchip(xhat0,yhat0);
pp{i}.V=fnint(pp{i}.SA);
end

%% find surface areas
idx=find(H0==9999); %which lakes are full
totSA=zeros(numel(H0),1);
V=zeros(numel(H0),1);
for i=1:numel(idx)
totSA(idx(i))=ppval(pp{i}.SA,pp{i}.SA.breaks(end));
V(idx(i))=ppval(pp{i}.V,pp{i}.V.breaks(end));
end

idx=idx(end)+1; %which lakes are full
totSA(idx)=ppval(pp{idx}.SA,H0(idx));
V(idx)=ppval(pp{idx}.V,H0(idx));
FE = totSA.*E; %evaporation flux
FIN=flipud(cumsum(flipud(FE))); %lake input fluxes
FOUT=FIN-FE; %lake output fluxes
```

d18_sim.m

```
function [time,d18out,C]=d18_sim(E,H,d18p,d18L,dt,yrs,thin)

[FIN,FE,FOUT,V]=height2F(H,E);
d18=[d18p;d18L];
iter=yrs*365*24*3600./dt;
iter=ceil(iter);


ktot=find(V>0,1,'last');
time=(0:dt*thin:dt*iter)';
time=time./365./24./3600;
d18out=NaN(ktot,numel(time));
d18out(:,1)=d18(2:ktot+1);

count=0;
record=1;
for i=1:iter
    count=count+1;
    for k=ktot:-1:1
```

```
        d18(k+1)=(V(k)*d18(k+1)+FIN(k)*d18(k)*dt-FE(k)*(d18(k+1)-
10)*dt-FOUT(k)*d18(k+1)*dt)./V(k);%changed to *(d18(k+1)-6)for
scenario B and *(d18(k+1)-14)for scenario C
    end

    if count==thin
        count=0;
        record=record+1;
        d18out(:,record)=d18(2:ktot+1);
    end
end

%convergence check
for k=1:ktot
    C(k)=FIN(k)*d18(k)-FE(k)*(d18(k+1)-10)-FOUT(k)*d18(k+1);% changed
to *(d18(k+1)-6)for scenario B and *(d18(k+1)-14)for scenario C
end
```

d18_sim_cutoff.m

```
function [timeout,d18out,Hout]=d18_sim_cutoff(E,H0,d18L,dt,yrs,thin)

load lake_splines
pp.SA=Mungo.SA;

%% add static head to lake Mungo
z=1; %add 1 metre
xhat=pp.SA.breaks;
yhat=ppval(pp.SA,xhat);
dz=xhat(2)-xhat(1);
xhat0=[xhat,(xhat(end)+dz:dz:xhat(end)+z)];
dSA=ppval(fnder(pp.SA),xhat(end));
yhat0=[yhat,yhat(end)+(dz:dz:z)*dSA];
pp.SA=pchip(xhat0,yhat0);
pp.V=fnint(pp.SA);

%define starting height
if H0(1)==9999
    H=pp.SA.breaks(end);
else
    H=H0(1);
end

%define finishing height
H1=H0(2);
if H1<0.1;
    H1=0.1;
end
```

```
%define lake heights
Hi=(H:-dt*E:H1-dt*E)';
Vi=ppval(pp.V,Hi);

%set initial state
d18=d18L;
timeout=NaN(ceil(numel(Hi)./thin),1);
d18out=timeout;
Hout=timeout;
timeout(1)=0;
d18out(1)=d18L;
Hout(1)=Hi(1);

count=0;
record=1;
for i=1:numel(Hi)-1
    count=count+1;
    VE=Vi(i)-Vi(i+1); %volume of water evaporated
    d18=(Vi(i)*d18-VE*(d18-10))./(Vi(i)-VE);% changed to *(d18-6)for
scenario B and *(d18-14)for scenario C

    if count==thin
        count=0;
        record=record+1;
        timeout(record)=i*dt;
        d18out(record)=d18;
        Hout(record)=Hi(i);
    end
end

idx=find(~isnan(timeout));
timeout=timeout(idx);
timeout=timeout./3600./24./365;
d18out=d18out(idx);
Hout=Hout(idx);
```

d18_example1.m

```
%% Example 1
%(1)Set evaporation to Canberra mean value
%(2)Flood lakes with precipitation until Mungo is almost overflowing
(water height of 7.6554 m)
%(3)Iterate for 20 years to bring isotopes effectively into
equilibrium
%(4)Reduce the water flux to bring the water height of Mungo to 0.5 m
%(5)Iterate for 20 years to bring isotopes effectively into
equilibrium

%% clear memory and close all figures
clear all, close all
```

```
%% define Canberra mean annual evaporation
E=1825; %[mm/yr]
E=E./1000./365./24./3600; % [m/s]

%% setup iteration scheme
dt=100; %time step in seconds
yrs=20; %number of years to calculate
thin=200; %only record every 200th time step

%% set oxygen isotope values [per mil]
d18p=-8; %value of precipitation
d18L=ones(5,1)*d18p; %set 5 lakes to have precipitation value

%% fill lakes with precipitation and iterate towards equilibrium
H0=[9999 9999 9999 7.6554 0]; %set fixed lake heights (9999=full)
[time0,d18out0]=d18_sim(E,H0,d18p,d18L,dt,yrs,thin); %iterate

%% instantly reduce incoming flux to Mungo
H0=[9999 9999 9999 0.5 0]; %set fixed lake heights (9999=full)
d18L(H0>0)=d18out0(:,end); %final d18O values of previous run give
starting values
[time1,d18out1,C1]=d18_sim(E,H0,d18p,d18L,dt,yrs,thin); %iterate

%% plot results of both runs together
time=[time0;time1+time0(end)]; %combine time arrays
d18O=[d18out0,d18out1]; %combine isotope arrays
figure %create new figure
plot(time,d18O)
ylim=get(gca,'ylim'); %find the limits on the y-axis
hold on
plot(ones(1,2)*time0(end),ylim,'--k') %add dashed line to seperate
models
set(gca,'tickdir','out','xminortick','on','yminortick','on')
xlabel('Time [yrs]') %label the x-axis
ylabel('Lake \delta^{18}O [^o/_{oo}]') %label the y-axis
legend('Mulurulu','Garnpung','Leaghur','Mungo');

%% calculate efolding time
% for j=1:4
%     test=d18out1(j,:);
%     test=test-test(end);
%     test=test./test(1);
%     e=[0.5:0.1:3];
%     for i=1:numel(e)
%         ef(i)=invinterp1(time1,test,1/exp(e(i))./e(i);
%     end
%     ef_bar(j)=mean(ef);
% end
```

d18_example2.m

```
%% Flood, balance and evaporation Model
%(1)Set evaporation to location value
%(2)Flood lakes with precipitation until Mungo is almost overflowing
(water height of 7.6554 m)
%(3)Iterate for 20 years to bring isotopes effectively into
equilibrium
%(4a)Reduce the water flux to cut-off Mungo
%(4b)Set evaporation to location value
%(4c)Set target water height for Mungo
%(5)Iterate isotopes until Mungo evaporates to target water height

%% clear memory and close all figures
clear all, close all

%% define location evaporation - first 20 years
Ew=800; %[mm/yr] change to 800 for Winter, 3600 for Summer
Ew=Ew./1000./365./24./3600; %[m/s]%% define location evaporation

%% define location evaporation - after cut off
Es=800; %[mm/yr] change to 800 for Winter, 3600 for Summer
Es=Es./1000./365./24./3600; %[m/s]

%% setup iteration scheme
dt=100; %time step in seconds
yrs=20; %number of years to calculate
thin=200; %only record every 200th time step

%% set oxygen isotope values [per mil]
d18p=-8; %value of precipitation
d18L=ones(5,1)*d18p; %set 5 lakes to have precipitation value

%% fill lakes with precipitation and iterate towards equilibrium
H0=[9999 9999 9999 7.6554 0]; %set fixed lake heights (9999=full)
[time0,d18out0]=d18_sim(Ew,H0,d18p,d18L,dt,yrs,thin); %iterate

%% cutoff Mungo and evaporate at set evaporative rate
H0=[7.6554 0.1]; %starting water height and final water height
d18L=d18out0(4,end); %final Mungo d18O value of previous run gives
starting value
[time1,d18out1]=d18_sim_cutoff(Es,H0,d18L,dt,yrs,thin); %iterate

%% plot results
figure %create new figure
plot(time0,d18out0); %plot initial set of results
hold on
cmap=get(gca,'colororder'); cmap=cmap(4,:); %find the Mungo line color
plot(time1+time0(end),d18out1,'-','color',cmap) %add Mungo evaporation
record
%ylim=get(gca,'ylim'); %find limits on y-axis
plot(ones(1,2)*time0(end),ylim,'--k') %add dashed line to seperate
models
set(gca,'tickdir','out','xminortick','on','yminortick','on')
```

```
xlabel('Time [yrs]') %label the x-axis
ylabel('Lake \delta^{18}O [^o/_{oo}]') %label the y-axis
legend('Mulurulu','Garnpung','Leaghur','Mungo');
grid minor %add minor gridlines
ylim([-10 60])
```

Table 1: scenarios run using the steady state model, evaporation rates are from the Bureau of Meteorology (2020b).

Scenario	**Parameters**
A	Starting water value: - 8 ‰ Evaporation rate = 2000 mm/yr X in equation 4 = 10 (equilibrium conditions)
B	Starting water value: - 8 ‰ Evaporation rate = 2000 mm/yr X in equation 4 = 6 (kinetic effects)
C	Starting water value: - 8 ‰ Evaporation rate = 2000 mm/yr, X in equation 4 = 14 (kinetic effects)
D	Starting water value: - 8 ‰ Evaporation rate = 800 mm/yr (Winter evaporation) X in equation 4 =10 (equilibrium conditions)
E	Starting water value: - 8 ‰ Evaporation rate: 3600 mm/yr (Summer evaporation) X in equation 4 =10 (equilibrium conditions).

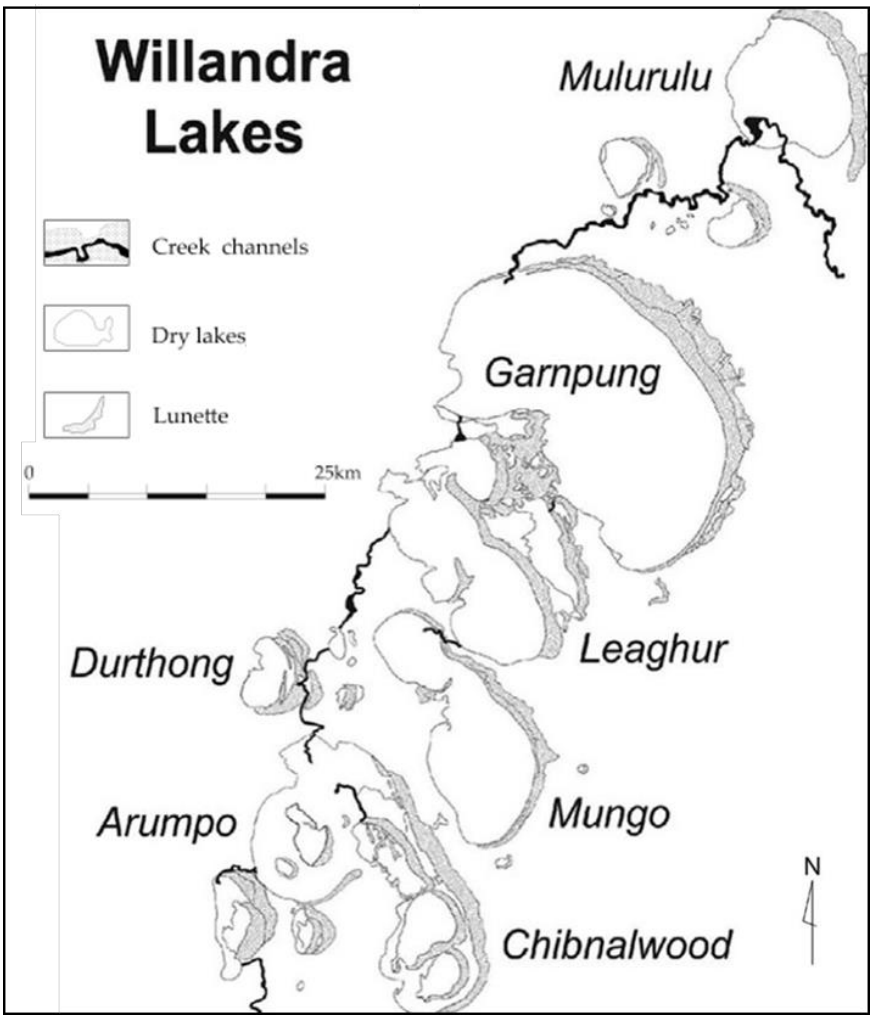

Figure 1

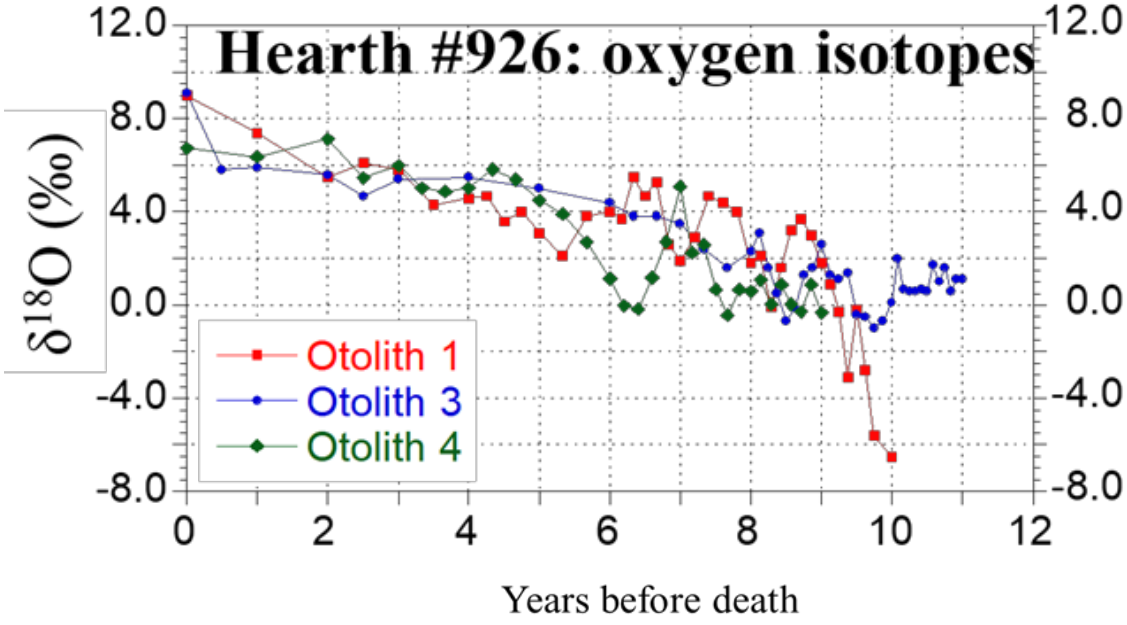

Figure 2

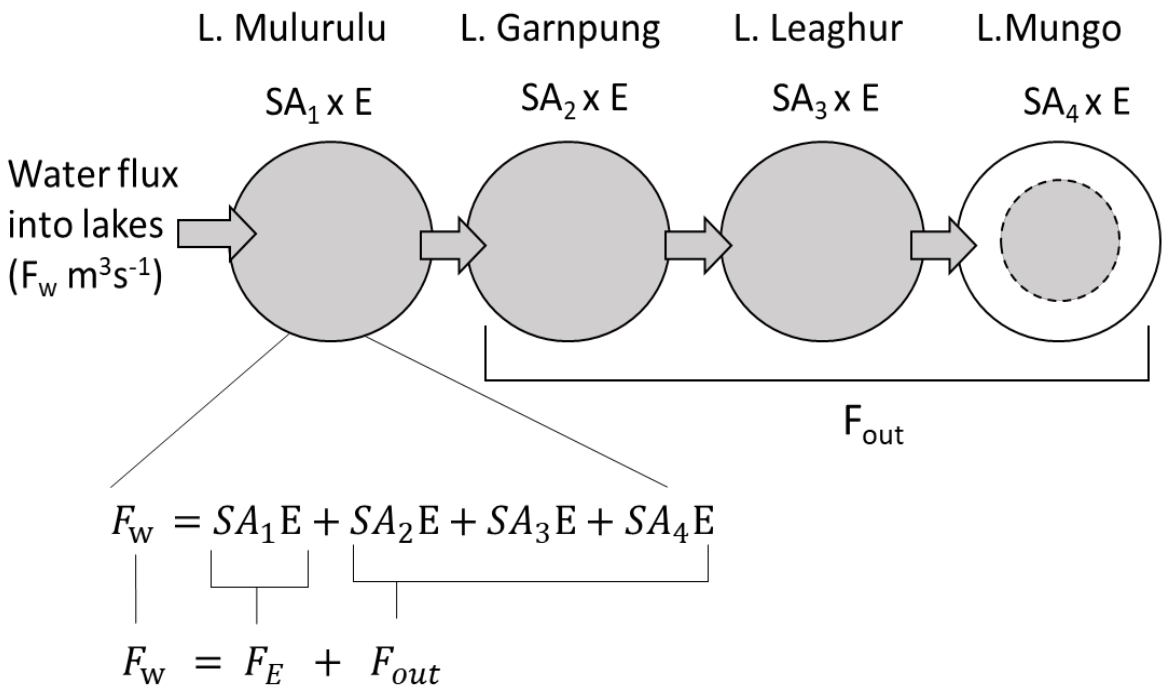

$$F_{\mathrm{w}} = SA_1\mathrm{E} + SA_2\mathrm{E} + SA_3\mathrm{E} + SA_4\mathrm{E}$$

$$F_{\mathrm{w}} = F_E + F_{out}$$

F_w is the water flux entering the lakes
F_E is the flux of water lost to evaporation
F_{out} is the water flux that flows out to the next lake

$F_w = F_E + F_{out}$ (Water level maintained)
$F_w < F_E$ (Water level lowers)
$F_w > F_E$ (Water level rises)

Figure 3

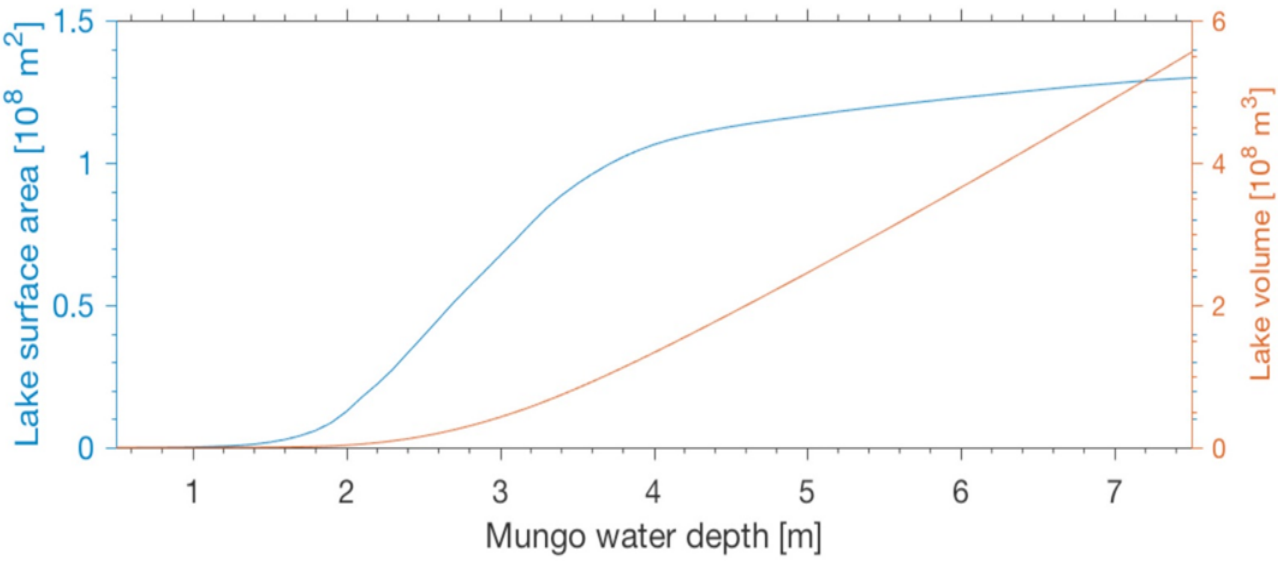

Figure 4

Figure_5

Click here to access/download;Figure;Figure_5.pdf

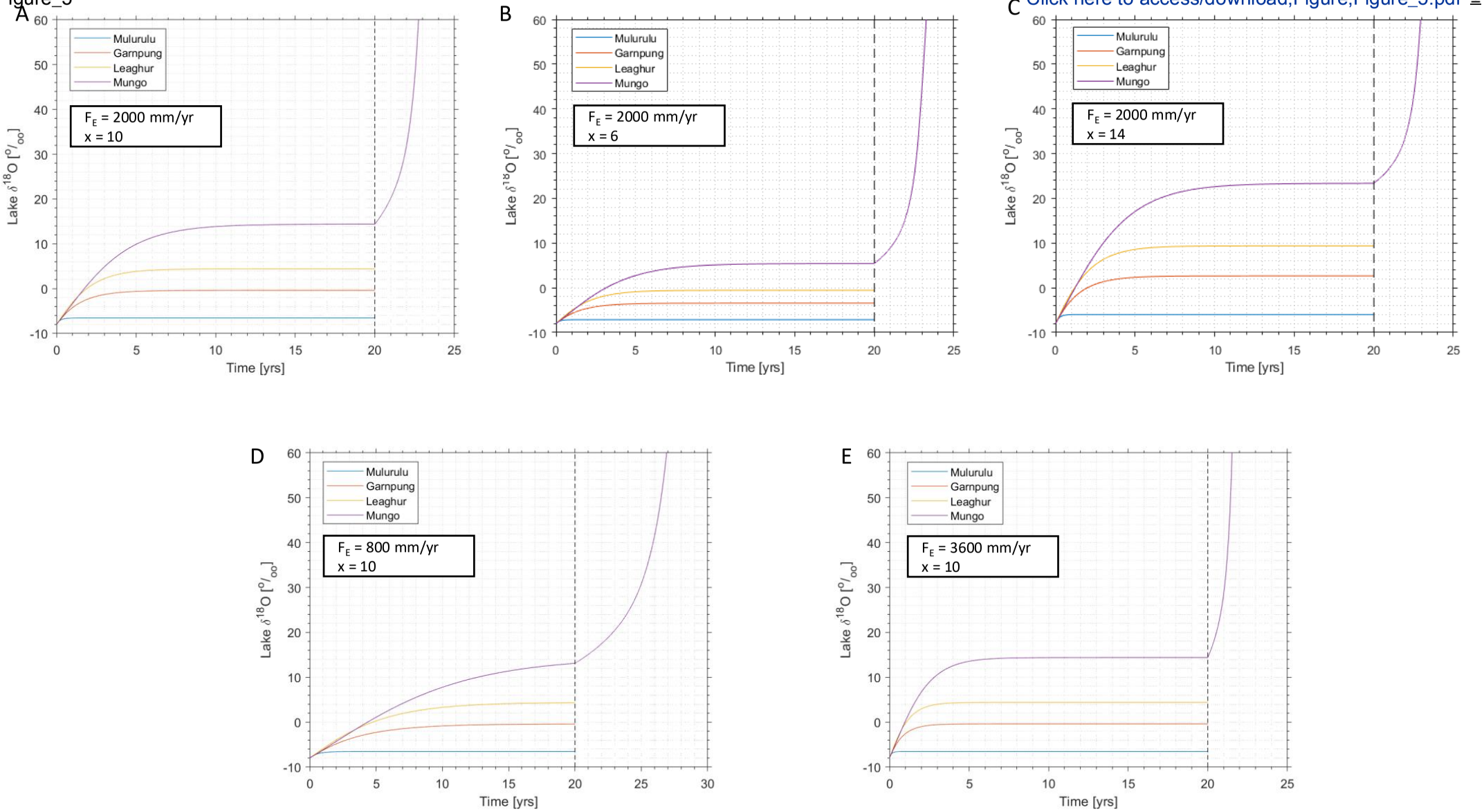

Figure 5